The Cryosphere Discuss., doi:10.5194/tc-2016-227, 2016
Manuscript under review for journal The Cryosphere
Published: 14 October 2016

The Cryosphere Discussions
Open Access
EGU

Numerical modelling of convective heat transport by air flow in permafrost-affected talus slopes

Jonas Wicky[1], Christian Hauck[1],

[1]Department of Geosciences, University of Fribourg, Fribourg, 1700, Switzerland

Correspondence to: Jonas Wicky (jonas.wicky@unifr.ch)

Abstract. Talus slopes are a widespread geomorphic phenomenon in the Alps. Due to their high porosity a gravity-driven internal air circulation can be established which is forced by the gradient between outside (air) and internal (talus) temperature. The thermal regime is different from the surrounding environment often leading to cold microclimates and permafrost occurrences. So far this phenomenon has mainly been analysed by field studies and only few explicit modelling studies of this phenomenon exist. Numerical simulations of permafrost sometimes use parameterizations for the effects of convection, but mostly neglect the influence of convective heat transfer in air on the thermal regime. On the contrary, in civil engineering many studies were carried out to investigate the thermal behaviour of blocky layers and to improve their passive cooling capacity. The present study further develops and applies these concepts to model heat transfer in air flow in a natural scale talus slope. Modelling results show that convective heat transfer has the potential to develop a temperature difference between the lower and the upper part from about 0.7°C (boundary closed to the atmosphere) to 2.5°C (boundary open to the atmosphere). A seasonally alternating chimney-effect type circulation develops. Modelling results also show that this convective heat transfer leads to a cold reservoir in the lower part of the talus slope which can be crucial for maintaining the frozen ground conditions under climate change.

1 Introduction

Mountain permafrost is currently undergoing substantial changes due to climate change as a whole and especially due to the observed and projected air temperature increase. Among the typical mountain permafrost substrates, i.e. rock, fine sediments and coarse blocky surfaces, the latter play an important role because of their high insulating characteristics for the subsurface underneath due to the low thermal conductivity of the air voids between the blocks (Harris and Pedersen 1998, Herz et al. 2003, Juliussen and Humlum 2008). In addition, air convection with upward transport of warmer air from the permafrost body and downward transport of cold air from the surface can take place within the coarse blocky layer, both, vertically (in flat terrain) as well as in form of a 2-dimensional slope circulation. These two effects lead first of all to much colder surface and subsurface temperatures for surfaces with coarse blocky surface layers compared to fine-grained or bedrock surfaces (e.g. Hanson and Hölzle 2004, Schneider et al. 2012, Gubler et al. 2011), but in consequence also to persisting permafrost occurrences at the lower limit of permafrost (including rock glaciers and ice-cored moraines) and specifically to sporadic or

The Cryosphere Discuss., doi:10.5194/tc-2016-227, 2016
Manuscript under review for journal The Cryosphere
Published: 14 October 2016

azonal permafrost occurrences at low altitudes (e.g. Kneisel et al. 2000, Gude et al. 2003, Delaloye et al. 2003, Kneisel et al. 2015). For the latter, mean annual air temperatures are positive and no permafrost would exist without this effect. These permafrost occurrences occur mostly in form of undercooled scree/talus slopes and have been well researched in a number of publications (Funk and Hoelzle 1992, Wakonigg 1996, Kneisel et al. 2000, Gude et al. 2003, Sawada et al. 2003, Delaloye et al. 2003, Gorbunov et al. 2004, Delaloye and Lambiel 2005, Zacharda et al. 2007, Morard and Delaloye 2008, Morard et al. 2008, Phillips et al. 2009, Gądek and Leszkiewicz 2012, Stiegler et al. 2014, Kneisel et al. 2015).

Previous review articles about mountain permafrost research have highlighted the need for improved process understanding and model studies for the complex subsurface material of Alpine terrain (Harris et al. 2009, Haeberli et al. 2010, Etzelmüller 2013). Whereas the energy balance for the coarse blocky surface layer of rock (and debris-covered) glaciers and talus slopes has been addressed in several field and modelling studies (e.g. Hanson and Hoelzle 2004, Scherler et al. 2014, Reid and Brock 2010), the effect of the internal 2-dimensional air circulation driven by the gradient between outside (air) and internal (talus) temperature has not been treated in detail or quantified with respect to the other terms in the energy balance. Transient numerical simulations of permafrost usually neglect the influence of convective heat transfer in air on the thermal regime or parameterize it with an apparent thermal conductivity (Gruber and Hoelzle 2008) or with an artificial heat sink (Scherler et al. 2013, 2014). Only very few and idealised modelling studies of the air circulation in undercooled talus slopes exist to date (e.g. Tanaka et al. 2000, 2006).

In contrast, many studies were carried out in civil engineering to investigate the thermal behaviour of artificial blocky layers (such as railroad embankments) and to improve their passive cooling capacity (e.g. Goering and Kumar, 1996, Cheng 2005, Cheng et al. 2007, Pham et al. 2008, Zhang et al. 2005, Arenson et al. 2006, 2007). In this study we will adapt the modelling concepts from civil engineering to investigate the feasibility of using a commercially available finite-element modelling software (GeoStudio) to explicitly model the 2-dimensional heat transfer by air flow within an idealised talus slope and to quantify the cooling effect with respect to different sensitivity parameter. The simulations are driven by observational data from the talus slope Lapires in the Western Swiss Alps (Delaloye and Lambiel 2005, Scapozza et al. 2015, Staub et al. 2015).

2 Theory and data

2.1 Conceptual model

Convective processes describe the transport of energy by a fluid, in the present case the transport of heat by air flow through the available pore space. This is in contrast to heat transport by conduction or radiation, which are other important processes for the energy balance within coarse blocky surface layers (Scherler et al. 2014). Convective processes are responsible for the specific (cold) temperature regime in undercooled talus and scree slopes. Balch described already in 1900 the asymmetry of seasonal air circulations in ice caves with gravity induced descending cold air in winter, and an absence of circulating air in summer (Balch 1900). Wakonigg (1996) described the so-called chimney effect in talus slopes, where a seasonally turning

The Cryosphere Discuss., doi:10.5194/tc-2016-227, 2016
Manuscript under review for journal The Cryosphere
Published: 14 October 2016

air circulation produces descending cold air in summer and ascending warm air in winter. The corresponding cold air exits at the foot of the slope in summer and warm air exits (melt holes in the snow cover) at the top of the slope in winter have been observed in field studies at various talus and scree slopes (e.g. Gude et al. 2003, Sawada et al. 2003, Delaloye 2003, Delaloye et al. 2003, Zacharda et al. 2005, Zacharda et al. 2007, Morard et al. 2008, Lambiel and Pieracci 2008, Morard, 2011).

Figure 1 shows this process schematically in its most basic form (Morard et al. 2010). Here, the material composition within the talus slope is assumed to be homogeneous and the induced air circulation is most effective when the temperature gradient between the outside air (T_{ao}) and the voids in the porous substrate (T_{ai}) is large and if the voids between the blocks have a high connectivity. In reality the distribution of permafrost in talus slopes is often more complex, as material composition can be heterogeneous which means that the cooling effect is not affecting the whole talus slope in the same way (Delaloye and Lambiel 2005). In any case, the internal air circulation can lead to rapid ground cooling within a short amount of time, in particular at the bottom of the talus slope, where cold air is aspirated in winter.

Model studies trying to explicitly simulate this process are rare. Tanaka et al. (2000) investigated the air circulation at two sites (Ice Valley, Korea, and Nakayama, Japan) using field data, and analytical and numerical models. In their most complex 2-dimensional model they could confirm that the cooling effect in summer stems indeed from a gentle katabatic flow in stable stratified conditions, whereas the winter circulation is due to an unstable convective overturning with a convection cell of around 50m extension. In a 1-dimensional study of the energy balance within the coarse blocky surface layer of a rock glacier, Scherler et al. (2014) could estimate the impact of this seasonal varying convective heat transfer (heat source in winter, heat sink in summer) in comparison with other elements of the energy balance, and therefore also a comparison with observed data. However, this approach does not treat the underlying process and prohibits an explicit modelling of the 2-dimensional air circulation.

Convective heat transfer in permafrost context was explicitly modelled in several engineering studies. First numerical simulations were conducted by Goering & Kumar (1996) and showed a passive cooling effect of convective cells within coarse grained road embankments. The same effect, corresponding to a Rayleigh-Bénard circulation, was described by Guodong et al. (2007) as thermal semi-conductor which cools road or train embankments in permafrost regions in winter, whereas no heat can penetrate in summer, due to the stable temperature stratification within the coarse material. Further engineering studies (e.g. Arenson and Sego, 2006, Arenson et al. 2007, Pham et al. 2008, Pei et al. 2014) investigated and simulated these small-scale cooling effects to optimise passive cooling systems in permafrost regions.

In the following we will describe the model set-up for an explicit simulation of the larger and natural scale lateral heat transfer by two-dimensional air circulation within an alpine talus slope.

The Cryosphere Discuss., doi:10.5194/tc-2016-227, 2016
Manuscript under review for journal The Cryosphere
Published: 14 October 2016

2.2 Governing equations

The general heat flow equation including convective transfer by water and air can be formulated as follows (GeoStudio 2013a):

$$\left(\rho_s c_{ps} + Lw\frac{\partial W_u}{\partial T}\right)\frac{\partial T}{\partial t} = \frac{\partial}{\partial y}\left[K_t\frac{\partial T}{\partial y}\right] + c_{pa}\frac{\partial(\dot{m}_a T)}{\partial y} + \rho_w c_{pw}\frac{\partial(q_w T)}{\partial y} + Q \quad (1)$$

where

	L	latent heat of water [J m^{-3}]
	W_u	unfrozen water content [m^3 m^{-3}]
	w	volumetric water content [m^3 m^{-3}]
	T	temperature [K]
	y	coordinate(s) [m]
	K_t	thermal conductivity [W m^{-1} K^{-1}]
	Q	boundary flux [W m^{-3}]
	t	time [s]
	$\rho_{s/w}$	density soil/ water[g m^{-3}]
	c_{ps}	specific heat capacity soil [J g^{-1} K^{-1}]
	$c_{pa/pw}$	specific heat capacity air/water [J g^{-1} K^{-1}]
	$\dot{m}_a$	mass flow air [g s^{-1}]
	q_w	flow rate (Darcy) of water [m s^{-1}]

Water (Eq. 2) and air (Eq. 3) flow can be described as follows and have to be jointly solved, as air and water pressure are dependent variables (GeoStudio 2013b,c):

$$m_w\gamma_w\frac{\partial H_w}{\partial t} = \frac{\partial}{\partial y}\left[K_w\frac{\partial H_w}{\partial y}\right] + m_w\frac{\partial P_a}{\partial t} + Q_w \quad (2)$$

$$\left(\frac{\theta_a}{RT} + \rho_a m_w\right)\frac{\partial P_a}{\partial t} = \frac{\partial}{\partial y}\left[\frac{\rho_a K_a}{\gamma_{oa}}\frac{\partial P_a}{\partial y} + \frac{\rho_a^2 K_a}{\rho_{oa}}\right] - \left[\frac{\theta_a P_a}{R}\frac{\partial(\frac{1}{T})}{\partial t}\right] + [\rho_a\gamma_w m_w\frac{\partial H_w}{\partial t}] \quad (3)$$

where

	m_w	slope of the water storage curve[m s^2 g^{-1}]
	γ_w	unit weight of water [g m^{-2} s^{-2}]
	γ_{oa}	relative unit weight of water [g m^{-2} s^{-2}]

The Cryosphere Discuss., doi:10.5194/tc-2016-227, 2016
Manuscript under review for journal The Cryosphere
Published: 14 October 2016

H_w	total head [m]
K_w	hydraulic conductivity [m s^{-1}]
Q_w	boundary flux [s^{-1}]
K_a	air conductivity [m s^{-1}]
P_a	air pressure [Pa]
ρ_a	density of air [g m^{-3}]
ρ_{oa}	relative density of air [g m^{-3}]
θ_a	volumetric air content [m^3 m^{-3}]
R	specific heat capacity of dry air [J g^{-1} K^{-1}]

2.3 Forcing data sets

Forcing data are used from the talus slope Lapires which is situated at an altitude range of 2400–2700 m a.s.l. in the Valais Alps, Western Swiss Alps (e.g. Staub et al. 2015). Several long-term mean annual ground near surface temperature data series and several deep boreholes with respective temperatures measurements are available from this site (Delaloye and Lambiel 2005, Scapozza 2013, Scapozza et al. 2015, Staub et al. 2015), which is also part of the PERMOS network (Permafrost Monitoring Switzerland, www.permos.ch).

For this study we used ground surface temperature (GST) data as surface atmosphere boundary condition. Moreover, snow data from the nearby snow station Les Attelas (Swiss IMIS network) was used to model the seasonal decoupling of the ground from the atmosphere by the snow cover. Borehole temperature data was used to compare the modelled temperature distribution to the measured temperature series in the borehole.

Validation and ground truth data are available from four boreholes, both regarding temperature as well as material composition and layer structure of the sediments (Delaloye et al. 2001, Scapozza 2013, Scapozza et al. 2015) and geophysical measurements for the analysis of spatial heterogeneity (Delaloye 2004, Lambiel 2006, Hilbich et al. 2008, Hilbich 2010). The porosity within the permafrost layer ranges from 30 to 60% and is in some part of the talus slope mostly sealed by ice (Scapozza 2013, Hilbich 2010). The bedrock consists of gneiss and must be at least at 40m depth due to drilling results (Scapozza 2013, Scapozza et al. 2015).

3 Model setup

The commercially available software GeoStudio has already been applied to coarse blocky permafrost substrates in the context of different engineering purposes such as the investigation of the passive cooling effect in road embankments (Arenson et al. 2006) or the heat convection in coarse mine waste rock piles (Arenson et al. 2007). Furthermore, Mottaghy and Rath (2006) used it to validate their own model approach in a study of paleoclimate permafrost in porous media. In the

The Cryosphere Discuss., doi:10.5194/tc-2016-227, 2016
Manuscript under review for journal The Cryosphere
Published: 14 October 2016

engineering sciences modelling approaches of convective heat transport by air and the resulting passive cooling effect are numerous (e.g. Goering and Kumar 1996, Guodong et al. 2007, Lebeau and Konrad 2009). They were all able to show the important influence of convective heat transport on the ground thermal regime on a small scale.

In this study we pick up these concepts and adapt them to a natural scale talus slope. Within GeoStudio we use a finite element modelling approach that solves the partial differential heat equations including convective heat transfer over a 2-dimensional domain. The numerical domain is divided into sub-domains with different material properties (Fig. 2). Measured daily temperature values (see Sect. 2.3) were used as temperature forcing at the surface-atmosphere boundary for the transient modelling. This 2-dimensional approach allows an explicit modelling of the air flow and the resulting convective heat exchange over the spatial domain of a natural scale talus slope allowing to analyse its influence on the ground thermal regime.

3.1 Geometry (mesh)

Figure 2 shows the numerical domain with its four sub- domains. Each sub- domain represents a different material and has therefore different physical material properties (Sect. 3.2). The domain represents an idealised talus slope with a talus thickness of 17 m and a constant slope angle of 33°. An unstructured mesh of quadrilateral and triangular elements was used with a mesh size of 1.2 m in the talus decreasing to 3 m in bedrock and air domain. An adaptive time stepping scheme was used. The maximum time step is hereby 0.5 days, decreasing to 0.1 days until the Courant criterion is met (GeoStudio, 2013c). Convergence is met when the results of two different iterations differ by less than 0.01°C or do not differ by more than 0.1% for temperature and 0.001% for pressure. The maximum number of iterations was set to 30, and our experiments showed that the model runs numerically stable and produced interpretable results under these numerical conditions. Numerical configuration proved however to be a crucial and delicate point in defining the model boundaries and running the model.

3.2 Material properties

Table 1 summarises the material properties of the sub-domains shown in Fig. 2 which were used in our simulations. The heat conductivities and heat capacities are taken from Schneider (2014), who empirically established the different values for several periglacial landforms in the Murtèl-Corvatsch region. It can be assumed that these values are more accurate for natural-scale talus slopes than published values from laboratory experiments. The volumetric heat capacity for bedrock exposed at the surface is given by Schneider (2014) as 275 kJ $m^{-3}K^{-1}$ which is approximately eight times smaller than other published values for deep seated bedrock in permafrost (e.g. 1600 kJ $m^{-3}K^{-1}$ in Gruber and Hölzle 2008, > 2000 kJ $m^{-3}K^{-1}$ in Arenson and Sego 2006, 2000 kJ $m^{-3}K^{-1}$ in Nötzli et al. 2008, 2063 kJ $m^{-3}K^{-1}$ in Wegmann et al. 1998). Considering that the model is representing bedrock at depth and not at the surface the volumetric heat capacity is set to 2500 kJ $m^{-3}K^{-1}$. Arenson et al. (2006) point out, that the heat capacity has a less prominent influence on the temperature distribution than other parameters in Table 1, especially the air conductivity .

The Cryosphere Discuss., doi:10.5194/tc-2016-227, 2016
Manuscript under review for journal The Cryosphere
Published: 14 October 2016

The porosity is set to 0.5 for the material within talus slope. This value corresponds to measured porosity values in the drill cores (Scapozza et al. 2015) and model fitted values for the Lapires site (Marmy et al. 2016) as well as previously published studies for other coarse grained permafrost material (Gruber and Hölzle 2008, Scherler et al. 2014). The porosity of bedrock is assumed to be very small compared to the talus slope and is therefore set to a near-zero value for numerical reasons. The so-called air conductivity is a theoretical value of the potential air speed within the material. As Arenson et al. (2006) pointed out the chosen air conductivity has to be in accordance with the other numerical parameter settings (e.g. time step, mesh size) to guarantee numerical stability and convergence. In our study, the air conductivity in the bedrock was set to a near-zero value, assuming that no air circulates within the bedrock. The air conductivity within the talus and in the air was set to a value of 10^4 m day^{-1}. This value was obtained through numerical test simulations similar as in Arenson et al. (2007), who obtained the same value. Higher air conductivity values did not result in numerical convergence and lead to clearly unrealistic results. In comparison to the rock material, the heat capacity of the air above the surface is low. Air movement in the atmosphere and its influence on the talus are neglected in this simplified study. This is of course a simplification to real-world conditions, but helps to isolate the process of the internal air circulation within the talus slope without the existence of external forcing by wind.

Finally, the effect of snow is simulated in an indirect way. The thermal effect of snow on the ground is represented through the explicit GST boundary condition at the atmosphere-surface boundary. However, the decoupling of the subsurface from atmospheric circulation regarding the air flow is not represented by this boundary condition. To account for this de-coupling of air movement, the air conductivity above the surface is parameterised as a function of snow height. Snow height data from the IMIS station Les Attelas (in close proximity to the Lapires site with representative snow data, cf. Staub et al. 2015) was used to parameterise air conductivity. For a snow height lower than 0.2 m the snow layer does not restrict the circulation. From a snow height of 0.2m to 0.8m air conductivity linearly decreases from 10^4 to 0 m day^{-1} and thus makes the exchange between the air and the talus impossible for snow heights above 0.8 m (cf. Scherler et al. 2013). Morard (2011) have shown that air aspiration is also possible through the snow, but in general little is known about the characteristics and importance of this effect.

3.3 Boundary and initial conditions

The lower boundary condition is set to a constant value of + 0.6°C. Temperature data from the lowermost thermistor in the Lapires boreholes LAP_1108 at 39 m depth show values around + 0.6°C with no seasonal variability (PERMOS 2016). For the surface-atmosphere boundary condition a 13-year period (2000-2012) of the GST data series from the logger S15 at Lapires (cf. Sect. 2.3, see also Staub et al. 2015) is used. Initial conditions are set with a constant temperature of -0.2°C in the talus and 0.2°C in the surrounding bedrock followed by a seven years spin-up using the daily mean value from the above mentioned S15 GST data as forcing. After seven years a quasi-equilibrium state from the constant initial conditions is

The Cryosphere Discuss., doi:10.5194/tc-2016-227, 2016
Manuscript under review for journal The Cryosphere
Published: 14 October 2016

reached. After the seven years spin up procedure the 13-year data series is used at the atmospheric boundary as forcing to show the effects of interannual variability of the driving meteorological variables.

3.4 Model experiments

Simulations with four different model set-ups have been conducted (Table 2). The first set-up (CON) allows no air circulation at all and hence only conductive heat transfer is represented, as in most permafrost models and land-surface schemes. This set-up serves as reference simulation. The second setup (CLO) consists of a permanently closed domain which allows air circulation within the talus, but no exchange with the modelled air domain above the surface. In the third set up (OPE) exchange with the modelled air domain above the surface is always possible, whereas the fourth set up (SEA) allows only a seasonal circulation with the air block to represent the seasonal decoupling from talus and atmosphere by the snow cover.

4 Results

4.1 Air circulation

Figure 3 shows the simulated air circulation and temperature distribution in the full model domain for day 300 (beginning of winter) for the experiment with open boundary conditions between surface of the talus slope and atmosphere (OPE). The ascending air flow within the talus slope can be clearly seen with maximum flow velocities around 100 m day^{-1}, i.e. ~0.001 m s^{-1}, which is in the range of the values estimated in other model and observational studies (Tanaka et al. 2000). Meyer et al. (2016) estimated velocities of around 4m/minute (= 0.07 m s^{-1}) for air flow within an ice cave, which can be seen as the high porosity limit for this kind of intra-talus air circulation. The thermal effect of this circulation is clearly seen with positive temperatures around 2°C in the upper part of the talus slope and negative temperatures around -1°C in the lower part. Note that the near-surface layer shows homogeneously negative temperatures at this time of the year due to seasonal freezing from the surface, except for the exit region of the warm ascending air flow near 10 m horizontal distance in the upslope part.

The air circulation closes the circle via the atmosphere and aspires cold atmospheric air into the lower part of the talus slope, where also the minimum temperatures can be found (horizontal distance 110 m). This temperature distribution is a clear effect of the induced convective air circulation, as the pure conduction experiment (CON), which served as reference experiment and includes only heat conduction as thermal transfer process, shows a homogeneous temperature distribution (both spatially and temporally) except for a small layer close to the surface (not shown; see also the homogeneous results for the CON experiment in Fig. 6). Additionally, no negative temperatures and therefore no permafrost conditions are produced in this reference run.

Figure 4 shows the seasonal evolution of the air circulation shown in Fig. 3 regarding strength and direction for the different months. The seasonal reversal of the circulation, as postulated e.g. in Delaloye and Lambiel (2005) and Morard et al. (2010,

The Cryosphere Discuss., doi:10.5194/tc-2016-227, 2016
Manuscript under review for journal The Cryosphere
Published: 14 October 2016

cf. Fig. 1), is clearly visible with downslope air flow within the talus slope between June-September and ascending air circulation from November-May. The strongest circulation is hereby simulated in July-August whereas the winter circulation is less strong, but continues over a longer time period (7 months, in contrast to only 3-4 months in summer).

Figure 5 shows the differences of the simulated seasonal circulation depicted in Fig. 4 between the three experiments CLO, OPE and SEA. The seasons are hereby shown as 3-month averages regarding their typical conditions at high altitude, i.e.: winter – JFM; spring – AMJ; summer – JAS; autumn – OND. The transition period with reduced air circulation between April and June is seen in all experiments, however, it has to be noted that during these 3 months the circulation reverses (cf. Fig. 4) and downslope and upslope air flow will add to near-zero in a 3-month average. The strong downslope circulation in summer is seen in OPE and SEA, but much less so in CLO, as only little space in the near-surface part of the talus slope is available for the upward-directed backflow of air. In CLO the circulation is also weaker in winter, which clearly illustrates that an open boundary between atmosphere and talus slope is necessary to produce an air circulation of greater strength. However, it can be seen that also in CLO a seasonally reversing air circulation develops.

The OPE and SEA experiments differ regarding their open and seasonally closed boundary condition, the latter resembling the isolation effects of the seasonal snow cover. The comparison shows that between July – December almost no differences can be seen, as the snow cover is absent or not yet thick enough to dampen the air exchange between talus slope and atmosphere. On the contrary strong damping effects can be observed between January and June, corresponding to the presence of an up to 2 m thick snow cover (cf. Fig. 8).

4.2 Temperature

The effect of the seasonally reversible air circulation on the spatial temperature distribution was already shown in Fig. 3. Figure 6 shows the seasonal and interannual variations of this temperature effect for all four experiments. Looking at the temperature curves of the upper part of the talus slope (Node A), temperatures are always positive with a seasonal variability around 1°C. An exceptions can be seen e.g. for the summer 2003, where the effect of the exceptional heat wave (cf. Schär et al. 2004, Hilbich et al. 2008) can be clearly seen by a temperature increase between 1°C (CON) and 3°C (OPE and SEA). Apart from this anomalous year, interannual variability is small in the upper part of the talus slope. In addition, the effect of the snow cover (SEA A compared to OPE A) is small with no differences in summer and maximal temperature differences in winter of around 0.2°C.

In contrast, the interannual variability in the lower part of the talus slope is much more pronounced. Here, temperatures in the OPE and SEA experiment develop to show permafrost conditions which are almost conserved during the hot summer 2003. Temperature decreases of more than 3°C can be observed during the cold winters 2004/05 and 2005/06. After that, temperatures increase again steadily, but still show permafrost conditions at the end of the simulation period in 2012 for the OPE experiment.

Temperature differences between upper and lower part of the talus slope are up to 6°C during the warm and cold years 2003-2006, which is an effect of the air circulation alone, as no significant temperature differences were obtained in the conductive

The Cryosphere Discuss., doi:10.5194/tc-2016-227, 2016
Manuscript under review for journal The Cryosphere
Published: 14 October 2016

reference experiment (CON, grey and black line). Differences between the OPE and SEA experiments are around 0.2°C for the lower part of the talus slope, again showing the role of the snow cover for dampening the cooling effect of the talus slope circulation.

5. Discussion

The simulations shown above reproduce qualitatively the internal air circulation observed in low- and high altitude talus slopes and they are consistent with many different observational data sets. For a critical analysis of the reliability of the model approach and its results, the degree of realism of the processes in the model, its sensitivity to model parameters, a comparison with observed borehole temperatures in the talus slope Lapires as well as a discussion of the strength and weaknesses of the model will be addressed below.

5.1 Process analysis

Figure 7 shows the velocity of the air flow within the talus slope as a function of driving GST data. It is clearly seen that there is a strong correlation between large positive GST data and strong downslope (positive) air flow and correspondingly negative GST data with upslope (negative) air flow. This is in good accordance with the underlying process, where a large temperature gradient between inside and outside of the talus slope leads to ascending air if the interior is warmer than the outside, and descending air if the interior is colder than the outside air (Fig. 1). As the temperature within the talus slope is close to 0°C, a GST of 0°C corresponds roughly to zero movement as no temperature gradient is present. The high correlation coefficient (r^2) in the OPE and the SEA experiments shows that GST is a very important factor in explaining the air flow in the talus. The slightly lower r^2 in the CLO experiment is partly due to the weaker air circulation and thus greater influence of the values near the zero curtain, but may also indicates that the closed set up is a less adequate representation.

Figure 8 shows an analysis of the simulated air flow in dependence of the presence/absence of a snow cover for the three different experiments. As seen in the previous figures, the velocities are smallest for the CLO experiment, and the air flows downslope in summer and upslope in winter in all experiments. In addition, velocities in summer for OPE and SEA are identical as no snow cover is present. However, large differences can be seen in late autumn and during winter. Clearly, winter velocities are largest for OPE, as no snow cover inhibits the coupling between talus slope and atmosphere in this experiment. In contrast, maximal velocities for the ascending air flow are obtained in late autumn in the SEA experiment, which can be seen as the most realistic simulation, as it includes the non-linear damping effect of the snow cover. In late autumn, air (and also ground surface) temperatures can already be negative due to strong radiative cooling at the surface at night. In the absence of a thick snow cover (e.g. in autumn/early winter 2005, Fig. 8) a strong air circulation can develop, as the temperature gradient between interior and outside is large. As soon as the snow cover height reaches a completely isolating state, the air circulation is severely damped as can be seen by the increasing and then flattening velocity curve in the SEA experiment. A similar, but much weaker effect can be seen in early summer when the snow cover thickness

The Cryosphere Discuss., doi:10.5194/tc-2016-227, 2016
Manuscript under review for journal The Cryosphere
Published: 14 October 2016

decreases again. But as the temperature gradient is much weaker during this snow melt period, its effect on the evolution of the air circulation is also much smaller.

5.2 Sensitivities

Sensitivity simulations with different slope angles showed a strong influence of the slope angle on the strength of the air circulation and therefore the temperature evolution. Not surprisingly, larger slope angles lead to higher velocities and larger temperature contrasts due to the stronger gravitational forces, as was also noted in previous studies (e.g. Guodong et al. 2007). Because the mesh geometry (cf. Fig. 2) changes with changing slope angles, the obtained temperature dependencies on slope angle cannot be compared quantitatively in a strict sense. In addition, the circulation pattern changes with increasing slope angle. For the simulations with comparatively large slope angle (such as the 33° depicted in Fig. 2, which was used in all simulations shown above) only one 2-dimensional advection cell is present with seasonal reversal of the flow direction (cf. Figs. 3-5). With decreasing slope angle this circulation cell not only decreases in strength, it is also complemented by additional 1-dimensional vertical convection cells, which do not extend over the full model domain (not shown). For slope angles smaller than around 5° the air flow is dominated by several individual small vertical convection cells.

Guodong et al. (2007) describe a similar relation between slope angle and circulation patterns in laboratory experiments. They found a minimal slope angle of 15° for connected advection cells and a dependence on the Rayleigh number for larger slope angles. In practice, and also in our model simulations, a clear distinction between advective and vertical convection cells is difficult to make, as usually a gradual transition between the two phenomena is observed. Using in-situ measurements, Hanson and Hölzle (2004) showed that for the case of rock glacier Murtèl, a comparatively flat rock glacier that contains large furrows and ridges which additionally inhibit the lateral air circulation, the vertical exchange of air is more important than advective processes. A thorough observation- and simulation-based analysis of these dependencies has, however, not been undertaken yet.

In addition, the model is very sensitive regarding the so-called air conductivity parameter introduced above. Arenson et al. (2006) concluded that finding a physically-consistent combination of air conductivity, and temporal and spatial discretisation poses the largest practical problem concerning numerical stability in soil temperature simulations. In our simulations only a narrow range of air conductivities allow for convergent calculations that produce convective circulation patterns for a given mesh and time step. Similar results were obtained in GeoStudio (2012a) and Arenson et al. (2007), which suggests that the air circulation should be used as calibration parameter wherever subsurface temperature data are available, especially as usually no in-situ air velocity measurements within the talus slope are available.

5.3 Comparison to borehole data

Finally, the idealised experiments discussed above can be compared to the observed temperature evolution in a borehole situated in the central part of the talus slope Lapires. Even though the driving GST values were taken from this talus slope,

The Cryosphere Discuss., doi:10.5194/tc-2016-227, 2016
Manuscript under review for journal The Cryosphere
Published: 14 October 2016

this comparison can only be qualitatively as no temperature calibration has been attempted in our model and several differences between our model setup and the real conditions exist. Most notably is hereby the presence of an massive ice core at Lapires (see e.g. Hilbich 2010, Scapozza et al. 2015), which was not included in our simulations for simplicity. Even though technical problems with the temperature measurements until 2010 prohibit a detailed analysis of the permafrost temperatures, permafrost conditions are clearly present with an active layer thickness between 4-6 metres (PERMOS 2016). On a first glance, the simulations are similar to the observed temperatures, however, a small cold bias in the model can be identified. Correspondingly, the modelled active layer thickness is smaller and the penetration depth of the winter cooling is larger than in the observations.

This may be due to several reasons. Firstly, the mean of the driving GST values of the logger LAP_S15 is colder than the mean of the uppermost temperature sensor in the borehole (cf. Staub et al. 2015). Secondly, the massive ice core influences the ground thermal regime regarding (i) the induced air circulation patterns by blocking the air flow in a central region of the talus between 4m and approximately 15m depth, (ii) its different thermal properties from the air/rock material of the simulated talus slope and (iii) the latent heat necessary for phase changes. Finally, due to numerical effectivity, the depth to the bedrock was chosen to be much shallower in the model than in reality (cf. Scapozza et al. 2015), which may have an additional effect on the observed discrepancies.

5.4 Models strength and weaknesses

Modelling the air circulation and thus the convective heat transfer within a talus slope is an important contribution to the understanding of the complex thermal regime of a talus slope. This is the strength of our model: the convective heat transfer is explicitly modelled in two dimensions, and it is a first step to an explicit description of this process in more sophisticated long term permafrost models where ventilation so far is neglected or parameterized (cf. Marmy et al. 2016, Luethi et al. 2016). Weaknesses foremost concern latent heat effects by melting/freezing of ice. The model domain in this study is assumed to be dry and hence no ice is building up. This allows assessing the influence of the convective heat transfer by air flow in an isolated way but neglect the interaction of water, ice and air. In ice-rich talus slopes this interaction surely plays an important role but was beyond the scope of this study and might be part of future model improvements. Previous studies on the effect of convective heat transfer in porous media in permafrost environments also neglect the influence of water flow and assume the numeric domain to be dry (Goering and Kumar 1996, Arenson et al. 2006, 2007, Guodong et al. 2007). Finally, the air block above the talus slope is a very simplified representation of the atmosphere. Modelling the atmospheric air flow explicitly, e.g. the effect of wind speed on the intra-talus circulation, would, however, increase the complexity of the model strongly.

6. Conclusion and outlook

A numerical study of convective heat transfer by air flow in a 2-dimensional talus slope model has been conducted. The results show that without forced convection a seasonally alternating circulation develops which leads to a convective heat transfer within the talus and thus to a cooling effect in the lower part of the talus slope. It therefore has a significant influence of the thermal regime in a talus slope. Sensitivity studies with a conduction only model showed that this cooling can be crucial to maintain the frozen state of the ground during the warm season under critical climate conditions. Furthermore, sensitivity studies using different atmospheric boundary conditions were conducted by simulating a closed-to-atmosphere boundary (CLO), and open-to-atmosphere boundary (OPE) and a seasonally closed-to-atmosphere boundary (SEA) to represent the seasonal decoupling by a snow cover. The results showed that an open-to-atmosphere boundary led to the most efficient cooling. Compared to a conduction only set up a cooling of 0.28 °C (CLO), 0.94°C (SEA) and 1.19°C (OPE) was found at node B in the lower part of the talus slope as mean value over the whole 13 years. Further sensitivity studies showed the dependence of strong cooling effects on a high air velocity in the ground as well as large slope angles. However, the circulation pattern does not change significantly in these cases.

So far this phenomenon has mainly been analyzed by field studies (e.g. Delaloye et al. 2003, Gude et al. 2003, Sawada et al. 2005) and the explicit modelling of this process now confirms their findings. For simplicity, we so far neglected the formation of ice, which may be a reasonable assumption for low-altitude, but not for high alpine talus slopes (Delaloye and Lambiel 2005, Morard et al. 2010, Hilbich 2010, Scapozza et al. 2015). This will have to be improved in a future study. Future work should therefore aim to model the internal air circulation for a specific site taking into account a more detailed structure like an impermeable ice core to get a better validation and site specific quantifications of the process. Furthermore efforts have to be made to understand the complex coupling of snow and air circulation within a talus slope.

Acknowledgements

This study was conducted within the SNF-Sinergia project TEMPS financed by the Swiss National Science Foundation (project n° CRSII2 136279) and the authors would like to thank all colleagues within the project for their valuable input during meetings and conferences. We would like especially to thank Dr. L. Arenson for sharing his experience with GeoStudio, and Dr. B. Staub and Prof. R. Delaloye for their valuable input regarding the Lapires talus slope. Data of the Lapires field site were thankfully provided by the PERMOS network (Permafrost Monitoring Switzerland).

References

Arenson, L. U. and Sego, D. C.: Considering convective air fluxes in the design of engineered structures in cold regions, in Proceedings of the 59th Canadian geotechnical conference and the seventh joint CGS/IAH-CNC groundwater specialty conference, pp. 1–8., 2006.

Arenson, L. U., Sego, D. C. and Newman, G.: The use of a convective heat flow model in road designs for Northern regions, in 2006 IEEE EIC Climate Change Technology, pp. 1–8., 2006.

Arenson, L. U., Pham, H.-N., Klassen, R. and Sego, D. C.: Heat convection in coarse waste-rock piles, pp. 1500–1507, Ottawa, Ontario, Canada. October–21-24., 2007.

Balch, E. S.: Glacieres, or Freezing Caverns, Allen Lane & Scott, Philadelphia., 1900.

Cheng, G.: A roadbed cooling approach for the construction of Qinghai–Tibet Railway, Cold Regions Science and Technology, 42(2), 169–176, doi:10.1016/j.coldregions.2005.01.002, 2005.

Delaloye, R.: Contribution à l'étude du pergélisol de montagne en zone marginale., PhD Thesis, University Fribourg, Fribourg., 2004.

Delaloye, R. and Lambiel, C.: Evidence of winter ascending air circulation throughout talus slopes and rock glaciers situated in the lower belt of alpine discontinuous permafrost (Swiss Alps), Norsk Geografisk Tidsskrift - Norwegian Journal of Geography, 59(2), 194–203, doi:10.1080/00291950510020673, 2005.

Delaloye, R., Reynard, E. and Lambiel, C.: Pergélisol et construction de remontées mécaniques: l'exemple des Lapires (Mont-Gelé, Valais)., Frost in der Geotechnik. Mitteilungen der Schweizerischen Gesellschaft für Boden- und Felsmechanik, 141, 103–113, 2001.

Delaloye, R., Reynard, E., Lambiel, C., Marescot, L. and Monnet, R.: Thermal anomaly in a cold scree slope (Creux du Van, Switzerland), in Proceedings of the Eight International Conference on Permafrost, vol. 2125, Balkema, Zurich., 2003.

Etzelmüller, B.: Recent Advances in Mountain Permafrost Research, Permafrost and Periglac. Process., 24(2), 99–107, doi:10.1002/ppp.1772, 2013.

Funk, M. and Hoelzle, M.: A model of potential direct solar radiation for investigating occurrences of mountain permafrost, Permafrost and Periglac. Process., 3(2), 139–142, 1992.

Gądek, B. and Leszkiewicz, J.: Impact of climate warming on the ground surface temperature in the sporadic permafrost zone of the Tatra Mountains, Poland and Slovakia, Cold Regions Science and Technology, 79–80, 75–83, doi:10.1016/j.coldregions.2012.03.006, 2012.

GeoStudio: Air Flow Modeling with AIR/W2012. An Engineering Methodology. September 2013 Edition, GEO-SLOPE International, Ltd., 2013a.

GeoStudio: Seepage Modeling with SEEP/W2012. An Engineering Methodology. September 2013 Edition, GEO-SLOPE International, Ltd., 2013b.

GeoStudio: Thermal Modeling with TEMP/W2012. An Engineering Methodology. September 2013 Edition, GEO-SLOPE International, Ltd., 2013c.

Goering, D. J. and Kumar, P.: Winter-time convection in open-graded embankments, Cold Regions Science and Technology, 24(1), 57–74, doi:10.1016/0165-232X(95)00011-Y, 1996.

Gorbunov, A. P., Marchenko, S. S. and Seversky, E. V.: The thermal environment of blocky materials in the mountains of Central Asia, Permafrost Periglac. Process., 15(1), 95–98, doi:10.1002/ppp.478, 2004.

Gruber, S. and Hoelzle, M.: The cooling effect of coarse blocks revisited: a modeling study of a purely conductive mechanism, in Proceedings of the Ninth International Conference on Permafrost, Faibanks, Alaska., 2008.

Gubler, S., Fiddes, J., Keller, M. and Gruber, S.: Scale-dependent measurement and analysis of ground surface temperature variability in alpine terrain, The Cryosphere, 5(2), 431–443, doi:10.5194/tc-5-431-2011, 2011.

Gude, M., Hauck, C., Kneisel, C., Krause, S., Molenda, R., Ruzicka, V. and Zacharda, M.: Evaluation of permafrost conditions in non-alpine scree slopes in Central Europe by geophysical methods, EGS-AGU-EUG Joint Assembly, Vol. 1, p. 8966, 2003.

Guodong, C., Yuanming, L., Zhizhong, S. and Fan, J.: The "thermal semi-conductor" effect of crushed rocks, Permafrost Periglac. Process., 18(2), 151–160, doi:10.1002/ppp.575, 2007.

Haeberli, W., Noetzli, J., Arenson, L., Delaloye, R., Gärtner-Roer, I., Gruber, S., Isaksen, K., Kneisel, C., Krautblatter, M. and Phillips, M.: Mountain permafrost: development and challenges of a young research field, Journal of Glaciology, 56(200), 1043–1058, doi:10.3189/002214311796406121, 2010.

Hanson, S. and Hoelzle, M.: The thermal regime of the active layer at the Murtèl rock glacier based on data from 2002, Permafrost Periglac. Process., 15(3), 273–282, doi:10.1002/ppp.499, 2004.

Harris, S. A. and Pedersen, D. E.: Thermal regimes beneath coarse blocky materials, Permafrost Periglac. Process., 9(2), 107–120, 1998.

Herz, T., King, L. and Gubler, H.: Microclimate within coarse debris of talus slopes in the alpine periglacial belt and its effect on permafrost, in Proceedings of the Eighth International Conference on Permafrost., pp. 383–387, Balkema, Zurich, 2003.

Hilbich, C.: Time-lapse refraction seismic tomography for the detection of ground ice degradation, The Cryosphere, 4(3), 243–259, doi:10.5194/tc-4-243-2010, 2010.

Hilbich, C., Hauck, C., Hoelzle, M., Scherler, M., Schudel, L., Völksch, I., Vonder Mühll, D. and Mäusbacher, R.: Monitoring mountain permafrost evolution using electrical resistivity tomography: A 7-year study of seasonal, annual, and long-term variations at Schilthorn, Swiss Alps, J. Geophys. Res., 113(F1), F01S90, doi:10.1029/2007JF000799, 2008.

Juliussen, H. and Humlum, O.: Thermal regime of openwork block fields on the mountains Elgåhogna and Sølen, central-eastern Norway, Permafrost Periglac. Process., 19(1), 1–18, doi:10.1002/ppp.607, 2008.

Kneisel, C., Hauck, C. and Vonder Mühll, D.: Permafrost below the Timberline Confirmed and Characterized by Geoelectrical Resistivity Measurements, Bever Valley, Eastern Swiss Alps, Permafrost Periglac. Process., 11(4), 295–304, doi:10.1002/1099-1530(200012)11:4<295::AID-PPP353>3.0.CO;2-L, 2000.

Kneisel, C., Emmert, A., Polich, P., Zollinger, B. and Egli, M.: Soil geomorphology and frozen ground conditions at a subalpine talus slope having permafrost in the eastern Swiss Alps, CATENA, 133, 107–118, doi:10.1016/j.catena.2015.05.005, 2015.

Lambiel, C.: Le pergélisol dans les terrains sédimentaires à forte déclivité: distribution, régime thermique et instabilités, UNIL-Faculté des géosciences et de l'environnement-Institut de géographie, Lausanne., 2006.

Lambiel, C. and Pieracci, K.: Permafrost distribution in talus slopes located within the alpine periglacial belt, Swiss Alps, Permafrost Periglac. Process., 19(3), 293–304, doi:10.1002/ppp.624, 2008.

Lebeau, M. and Konrad, J.-M.: Natural convection of compressible and incompressible gases in undeformable porous media under cold climate conditions, Computers and Geotechnics, 36(3), 435–445, doi:10.1016/j.compgeo.2008.04.005, 2009.

Luethi R., Phillips M, Lehning M: Estimating non-conductive heat flow leading to intra-permafrost talik formation at Ritigraben rock glacier (Western Swiss Alps). Permafrost Periglac. Process., in press, 2016.

Marmy, A., Rajczak, J., Delaloye, R., Hilbich, C., Hoelzle, M., Kotlarski, S., Lambiel, C., Noetzli, J., Phillips, M. and Salzmann, N.: Semi-automated calibration method for modelling of mountain permafrost evolution in Switzerland, The Cryosphere, in press, 2016.

Meyer, C., Meyer, U., Pflitsch, A. and Maggi, V.: Analyzing airflow in static ice caves by using the calcFLOW method, The Cryosphere, 10(2), 879–894, doi:10.5194/tc-10-879-2016, 2016.

Morard, S.: Effets de la circulation d'air par effet de cheminée dans l'évolution du régime thermique des éboulis froids de basse et moyenne altitude, Université de Fribourg., 2011.

Morard, S., Delaloye, R. and Lambiel, C.: Time-lapse Electrical Resistivity Tomography (ERT) to estimate temperature changes at depth in a low elevation ventilated cold talus slope (Dreveneuse, Swiss Prealps), in Geophysical Research Abstracts, vol. 10., 2008.

Mottaghy, D. and Rath, V.: Latent heat effects in subsurface heat transport modelling and their impact on palaeotemperature reconstructions, Geophys. J. Int., 164(1), 236–245, doi:10.1111/j.1365-246X.2005.02843.x, 2006.

Noetzli, J., Hilbich, C., Hauck, C., Hoelzle, M. and Gruber, S.: Comparison of simulated 2D temperature profiles with time-lapse electrical resistivity data at the Schilthorn crest, Switzerland, in Proceedings of the Ninth International Conference on Permafrost, vol. 29, pp. 1293–1298, Faibanks, Alaska., 2008.

Pei, W., Zhang, M., Lai, Y., Jin, L. and Harbor, J.: Thermal stability analysis of crushed-rock embankments on a slope in permafrost regions, Cold Regions Science and Technology, 106, 175–182, doi:10.1016/j.coldregions.2014.07.005, 2014.

PERMOS: PERMOS Database. Swiss Permafrost Monitoring Network, Fribourg, Switzerland. DOI:10.13093/permos-2016-01, 2016.

Pham, H.-N., Arenson, L. U. and Sego, D. C.: Numerical analysis of forced and natural convection in waste-rock piles in permafrost environments, in Proceedings of the Ninth International Conference on Permafrost, Fairbanks, Alaska, 2008.

Phillips, M., Mutter, E. Z., Kern-Luetschg, M. and Lehning, M.: Rapid degradation of ground ice in a ventilated talus slope: Flüela Pass, Swiss Alps, Permafrost Periglac. Process., 20(1), 1–14, doi:10.1002/ppp.638, 2009.

Reid, T. D. and Brock, B. W.: An energy-balance model for debris-covered glaciers including heat conduction through the debris layer, Journal of Glaciology, 56(199), 903–916, doi:10.3189/002214310794457218, 2010.

Sawada, Y., Ishikawa, M. and Ono, Y.: Thermal regime of sporadic permafrost in a block slope on Mt. Nishi-Nupukaushinupuri, Hokkaido Island, Northern Japan, Geomorphology, 52(1–2), 121–130, doi:10.1016/S0169-555X(02)00252-0, 2003.

Scapozza, C.: Stratigraphie, morphodynamique, paléoenvironnements des terrains sédimentaires meubles à forte déclivité du domaine périglaciaire alpin, PhD Thesis, University Lausanne, Lausanne., 2013.

Scapozza, C., Baron, L. and Lambiel, C.: Borehole Logging in Alpine Periglacial Talus Slopes (Valais, Swiss Alps), Permafrost and Periglac. Process., 26(1), 67–83, doi:10.1002/ppp.1832, 2015.

Schär, C., Vidale, P. L., Lüthi, D., Frei, C., Häberli, C., Liniger, M. A. and Appenzeller, C.: The role of increasing temperature variability in European summer heatwaves, Nature, 427(6972), 332–336, doi:10.1038/nature02300, 2004.

Scherler, M., Hauck, C., Hoelzle, M. and Salzmann, N.: Modeled sensitivity of two alpine permafrost sites to RCM-based climate scenarios, J. Geophys. Res. Earth Surf., 118(2), 780–794, doi:10.1002/jgrf.20069, 2013.

Scherler, M., Schneider, S., Hoelzle, M. and Hauck, C.: A two-sided approach to estimate heat transfer processes within the active layer of the Murtèl–Corvatsch rock glacier, Earth Surface Dynamics, 2(1), 141–154, doi:10.5194/esurf-2-141-2014, 2014.

Schneider, S.: The heterogeneity of mountain permafrost–A fieldbased analysis of different periglacial materials, PhD Thesis, University of Fribourg, 176 pp., 2014.

Schneider, S., Hoelzle, M. and Hauck, C.: Influence of surface and subsurface heterogeneity on observed borehole temperatures at a mountain permafrost site in the Upper Engadine, Swiss Alps, The Cryosphere, 6(2), 517–531, doi:10.5194/tc-6-517-2012, 2012.

Staub, B., Marmy, A., Hauck, C., Hilbich, C. and Delaloye, R.: Ground temperature variations in a talus slope influenced by permafrost: a comparison of field observations and model simulations, Geographica Helvetica, 70(1), 45, doi:10.5194/gh-70-45-2015, 2015.

Stiegler, C., Rode, M., Sass, O. and Otto, J.-C.: An Undercooled Scree Slope Detected by Geophysical Investigations in Sporadic Permafrost below 1000 M ASL, Central Austria, Permafrost and Periglac. Process., 25(3), 194–207, doi:10.1002/ppp.1813, 2014.

Tanaka, H. L., Nohara, D. and Yokoi, M.: Numerical simulation of wind hole circulation and summertime ice formation at Ice Valley in Korea and Nakayama in Fukushima, Japan, Journal of the Meteorological Society of Japan, 78(5), 611–630, 2000.

Tanaka, H. L., Nohara, D. and Byun, H.-R.: Numerical Simulation of Wind Hole Circulation at Ice Valley in Korea Using a Simple 2D Model, Journal of the Meteorological Society of Japan. Ser. II, 84(6), 1073–1084, doi:10.2151/jmsj.84.1073, 2006.

Wakonigg, H.: Unterkühlte Schutthalden, Beiträge zur Permafrostforschung in Österreich. Arbeiten aus dem Institut für Geographie der Karl-Franzens-Universität Graz, 33, 209–223, 1998.

Wegmann, M., Gudmundsson, G. H. and Haeberli, W.: Permafrost changes in rock walls and the retreat of Alpine glaciers: a thermal modelling approach, Permafrost Periglac. Process., 9(1), 23–33, 1998.

Zacharda, M., Gude, M., Kraus, S., Hauck, C., Molenda, R. and Ružička, V.: The relict mite Rhagidia gelida (Acari, Rhagidiidae) as a biological cryoindicator of periglacial microclimate in European highland screes, Arctic, Antarctic, and Alpine Research, 37(3), 402–408, doi:10.1657/1523-0430(2005)037[0402:TRMRGA]2.0.CO;2, 2005.

Zacharda, M., Gude, M. and Růžička, V.: Thermal regime of three low elevation scree slopes in central Europe, Permafrost Periglac. Process., 18(3), 301–308, doi:10.1002/ppp.598, 2007.

Zhang, M., Lai, Y., Liu, Z. and Gao, Z.: Nonlinear analysis for the cooling effect of Qinghai-Tibetan railway embankment with different structures in permafrost regions, Cold Regions Science and Technology, 42(3), 237–249, doi:10.1016/j.coldregions.2005.02.003, 2005.

The Cryosphere Discuss., doi:10.5194/tc-2016-227, 2016
Manuscript under review for journal The Cryosphere
Published: 14 October 2016

Table 1: Material properties used for the GeoStudio simulations in this study (based on Schneider 2014, Arenson and Sego 2006, Arenson et al. 2007 and Scapozza et al. 2015, see text). The snow layer acts hereby only as idealised boundary that seasonally damps and prohibits air exchange between talus and atmosphere through coupling of the air conductivity value to the snow height. See text for further explanations.

material	thermal conductivity		specific heat capacity	vol. heat capacity	porosity	air conductivity
	[W $K^{-1}m^{-1}$]	[kJ day^{-1} m^{-1} K^{-1}]	[J kg^{-1} K^{-1}]	[kJ m^{-3} K^{-1}]		[m day^{-1}]
bedrock	2.4	207	99	2500	0.01	0.01
talus	1.2	103	904	1256	0.5	10^4
air	1.2	103	1	1.3	1	10^4
snow	1.2	129	1	1.3	1	$0 – 10^4$

Table 2: List and description of model experiments conducted.

Name	Processes included	Description
Conduction only (CON)	Conduction only	-
Closed (CLO)	Conduction and convection	No exchange with the air block
Open (OPE)	Conduction and convection	Unrestricted exchange with the air block
Seasonally closed (SEA)	Conduction and convection	Seasonally restricted exchange with the air block

The Cryosphere Discuss., doi:10.5194/tc-2016-227, 2016
Manuscript under review for journal The Cryosphere
Published: 14 October 2016

List of Figures:

The Cryosphere Discuss., doi:10.5194/tc-2016-227, 2016
Manuscript under review for journal The Cryosphere
Published: 14 October 2016

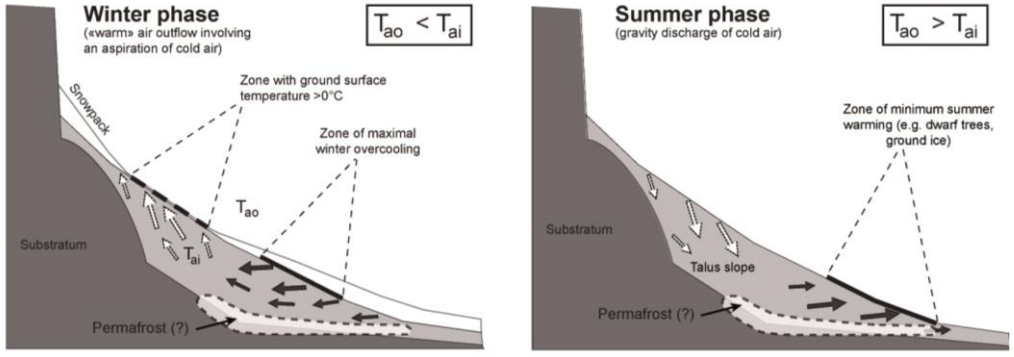

Figure 1: Schematic view of a seasonally alternating air circulation within a talus slope (modified from Morard et al. 2010). T_{ao} and T_{ai} denote air temperature outside and inside the blocky material, respectively.

The Cryosphere Discuss., doi:10.5194/tc-2016-227, 2016
Manuscript under review for journal The Cryosphere
Published: 14 October 2016

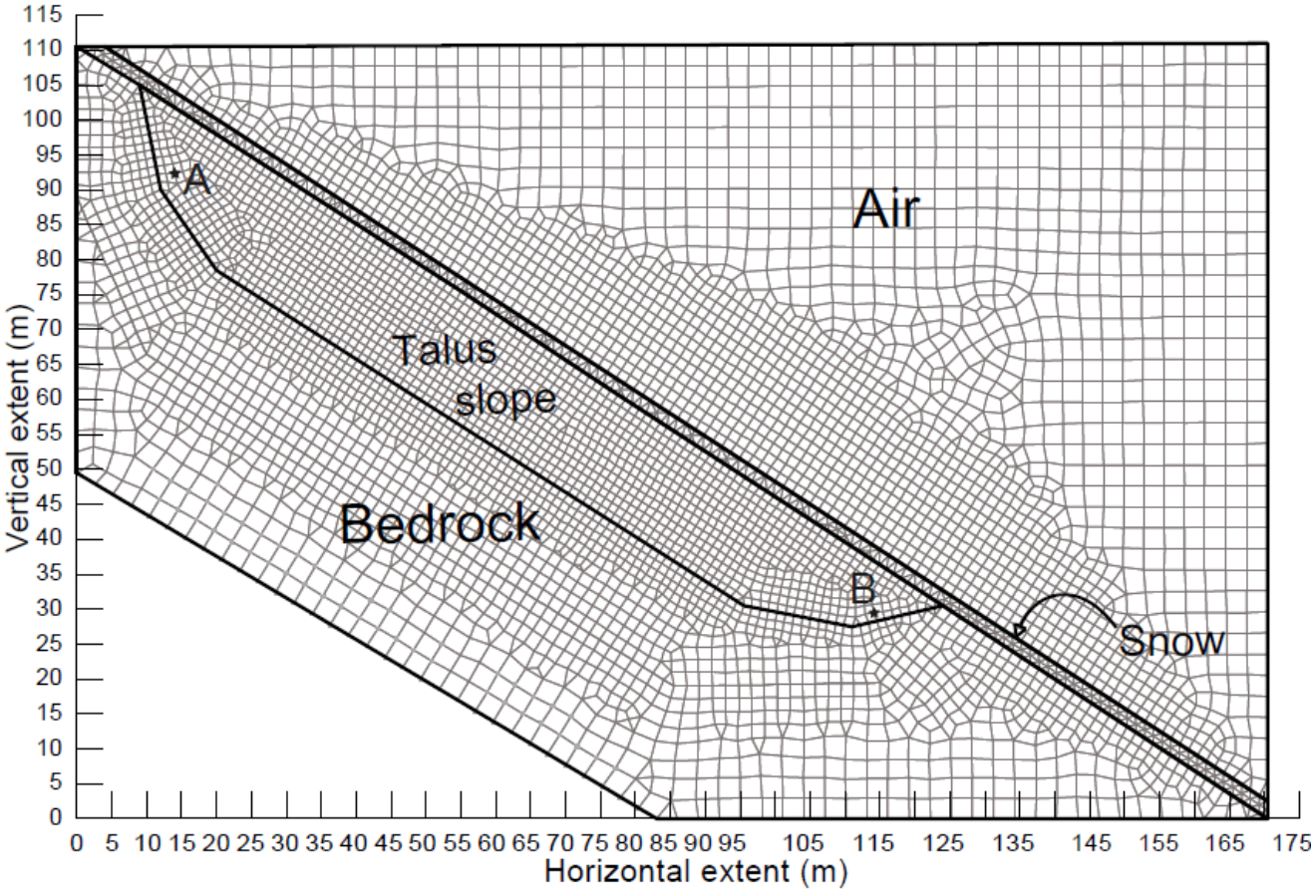

Figure 2: Model set-up and mesh showing the four sub-domains used in the talus slope experiments. The points (nodes) marked by A and B are reference points which will be further analysed in the following.

The Cryosphere Discuss., doi:10.5194/tc-2016-227, 2016
Manuscript under review for journal The Cryosphere
Published: 14 October 2016

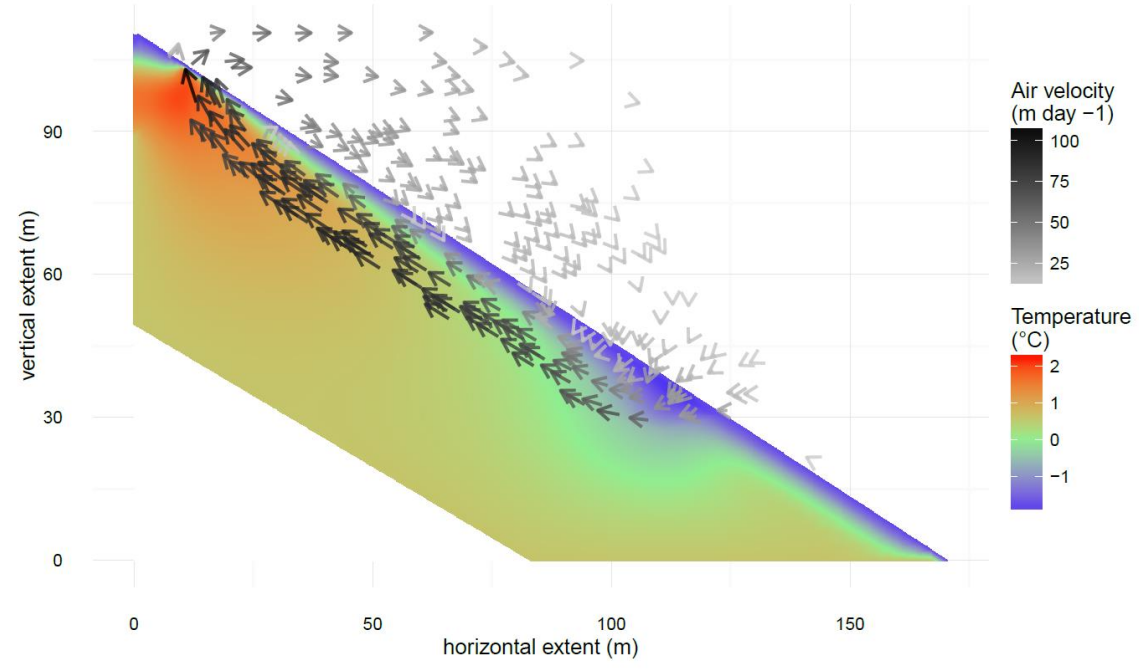

Figure 3: Simulated temperature distribution (colours) and air current vectors in the talus slope for the open experiment (OPE) for day 300 (winter circulation). The strength of the circulation is marked by the grey/black colour of the vector arrows and is given in m day^{-1}.

The Cryosphere Discuss., doi:10.5194/tc-2016-227, 2016
Manuscript under review for journal The Cryosphere
Published: 14 October 2016

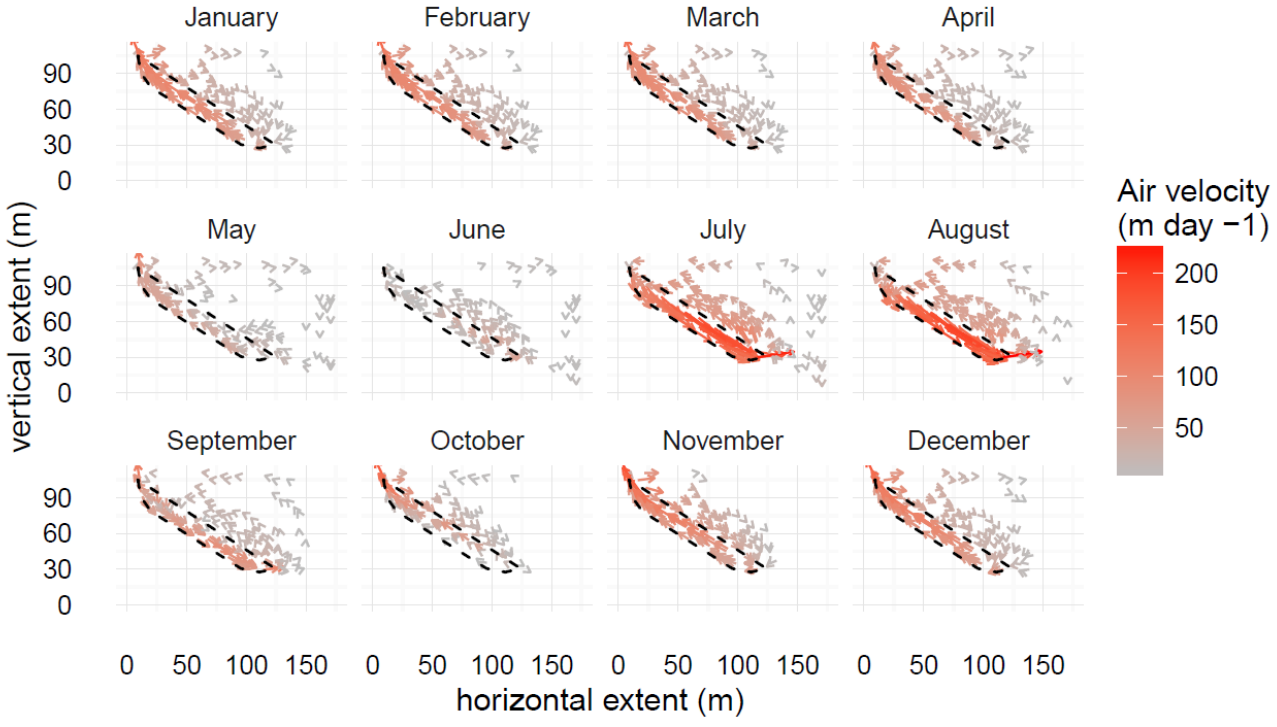

Figure 4: Mean monthly air flow of the open experiment (OPE) over the 13 modelled years. The dashed line marks the domain of the talus slope. The seasonal differences of the air circulation, both, regarding strength and direction, are clearly seen by the direction and colour of the arrows.

The Cryosphere Discuss., doi:10.5194/tc-2016-227, 2016
Manuscript under review for journal The Cryosphere
Published: 14 October 2016

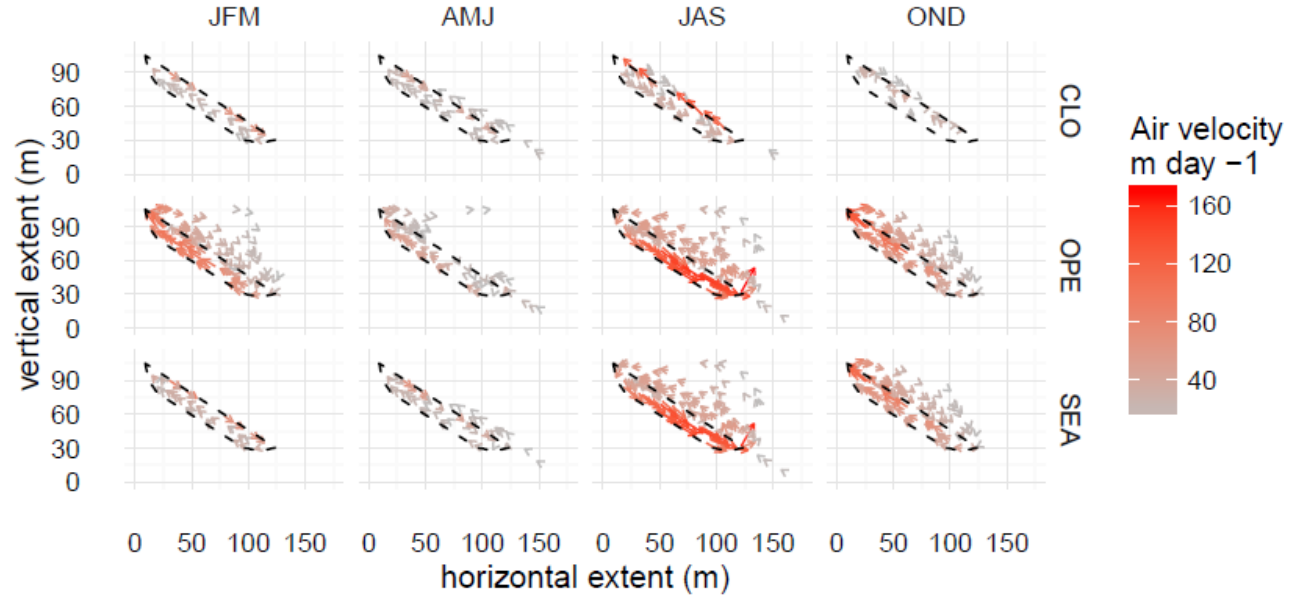

Figure 5: Modelled seasonal mean air flow for the modelled 13 years for the different atmospheric boundary conditions: (top) closed to atmosphere (CLO), (middle) open to atmosphere (OPE) and (bottom) seasonally closed to atmosphere (SEA). The talus slope is shown with the dashed line.

The Cryosphere Discuss., doi:10.5194/tc-2016-227, 2016
Manuscript under review for journal The Cryosphere
Published: 14 October 2016

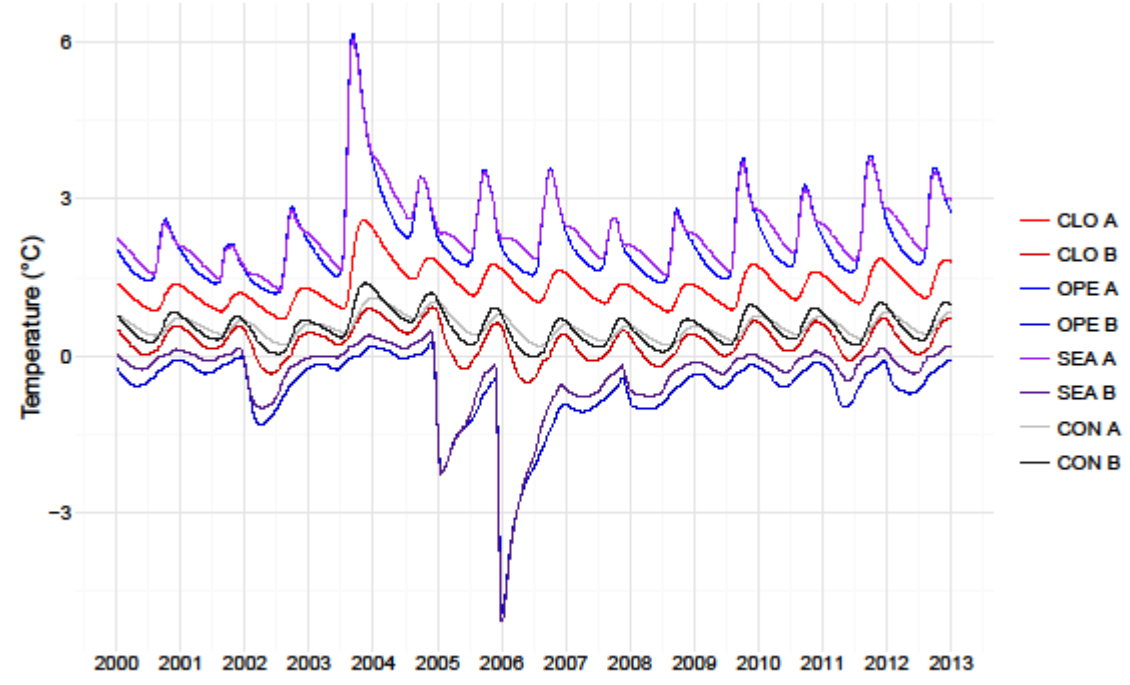

Figure 6: Temperature evolution at two different locations in the upper (node A, cf. Fig. 2) and lower (node B, cf. Fig. 2) part of the talus slope for the CLO (red), the OPE (blue), the SEA (purple) and the CON (black) experiment.

The Cryosphere Discuss., doi:10.5194/tc-2016-227, 2016
Manuscript under review for journal The Cryosphere
Published: 14 October 2016

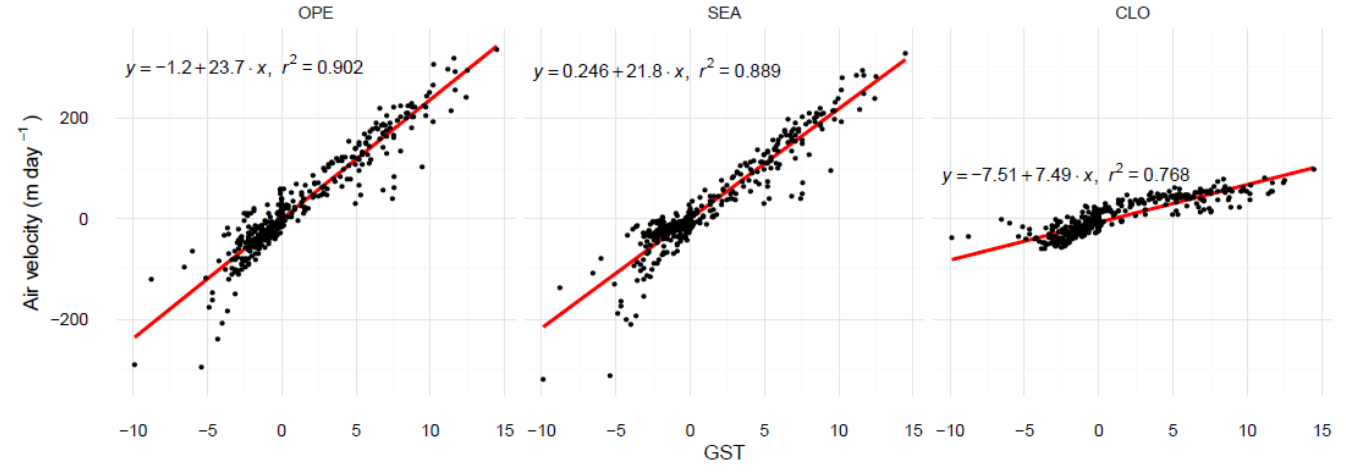

Figure 7: Relation between velocity of the air flow at node B (cf. Fig. 2) and the forcing ground surface temperature (GST) for the three different experiments OPE, SEA and CLO. Hereby, positive velocities indicate downslope movement and negative velocities indicate upslope movement.

The Cryosphere Discuss., doi:10.5194/tc-2016-227, 2016
Manuscript under review for journal The Cryosphere
Published: 14 October 2016

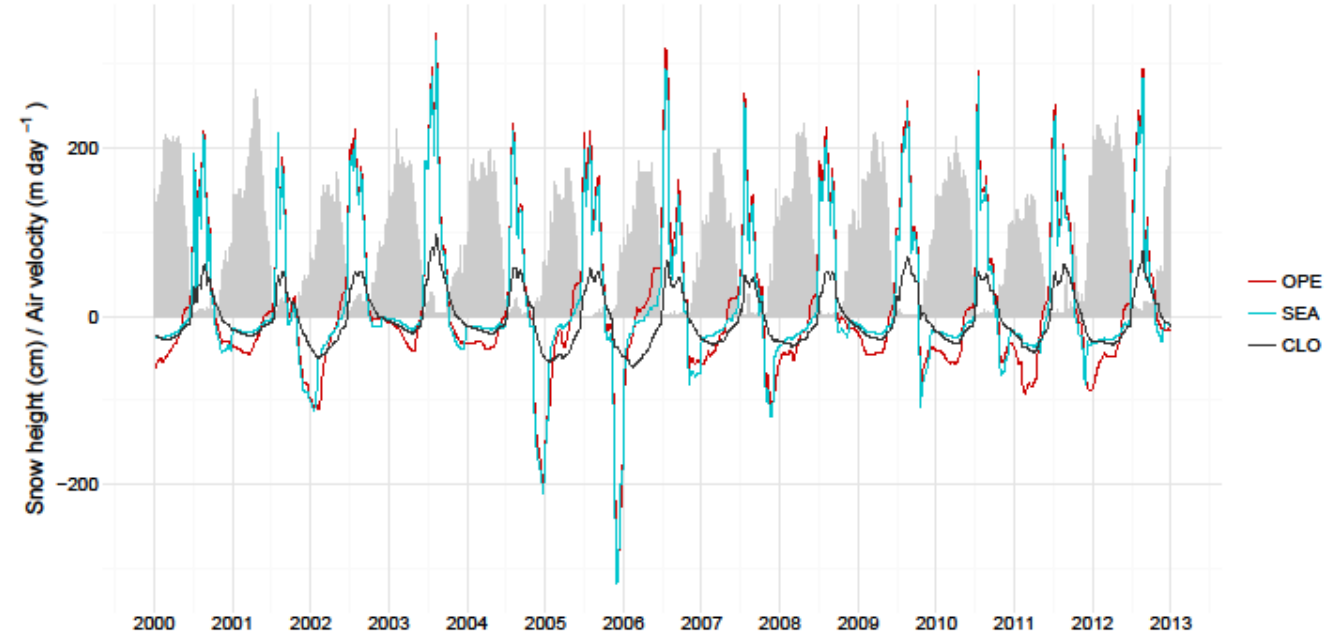

Figure 8: Velocity of the simulated air flow at node B (cf. Fig. 2) in the experiments OPE, SEA and CLO for the period 2010-2013 in relation to the presence of a snow cover (grey bars). Positive (negative) velocities correspond to downslope (upslope) air flow.

The Cryosphere Discuss., doi:10.5194/tc-2016-227, 2016
Manuscript under review for journal The Cryosphere
Published: 14 October 2016

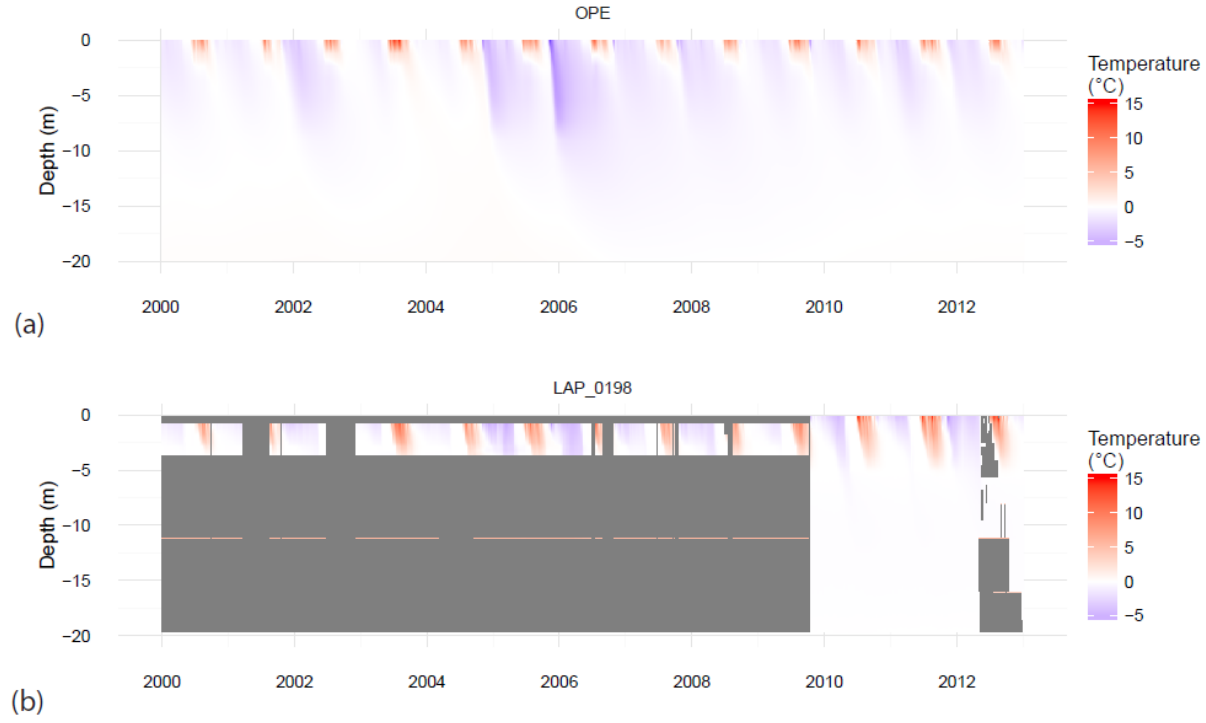

Figure 9: (a) Temperature plot along a perpendicular profile through node B for the OPE simulation for the 13 years period. (b) Borehole temperature from borehole LAP_0198 at the Lapires field site (PERMOS 2016). Missing values due to technical problems at larger depths are plotted in dark grey.